

UC Riverside

2016 Publications

Title

Understanding particles emitted from spray and wall-guided gasoline direct injection and flex fuel vehicles operating on ethanol and iso-butanol gasoline blends

Permalink

<https://escholarship.org/uc/item/44q9d99v>

Journal

Aerosol Science and Technology, 51(3)

ISSN

0278-6826 1521-7388

Authors

Short, Daniel
Vu, Diep
Chen, Vincent
[et al.](#)

Publication Date

2016-11-28

DOI

10.1080/02786826.2016.1265080

Peer reviewed




Understanding particles emitted from spray and wall-guided gasoline direct injection and flex fuel vehicles operating on ethanol and iso-butanol gasoline blends

Daniel Short, Diep Vu, Vincent Chen, Carlos Espinoza, Tyler Berte, Georgios Karavalakis, Thomas D. Durbin & Akua Asa-Awuku


To cite this article: Daniel Short, Diep Vu, Vincent Chen, Carlos Espinoza, Tyler Berte, Georgios Karavalakis, Thomas D. Durbin & Akua Asa-Awuku (2017) Understanding particles emitted from spray and wall-guided gasoline direct injection and flex fuel vehicles operating on ethanol and iso-butanol gasoline blends, *Aerosol Science and Technology*, 51:3, 330-341, DOI: [10.1080/02786826.2016.1265080](https://doi.org/10.1080/02786826.2016.1265080)

To link to this article: <https://doi.org/10.1080/02786826.2016.1265080>



 View supplementary material 

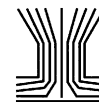
 Accepted author version posted online: 28 Nov 2016.
Published online: 18 Dec 2016.

 Submit your article to this journal 

 Article views: 581

 View Crossmark data 

 Citing articles: 5 View citing articles 



Understanding particles emitted from spray and wall-guided gasoline direct injection and flex fuel vehicles operating on ethanol and iso-butanol gasoline blends

Daniel Short^{a,b}, Diep Vu^{a,b}, Vincent Chen^{a,b}, Carlos Espinoza^{a,b}, Tyler Berte^{a,b}, Georgios Karavalakis^{a,b}, Thomas D. Durbin^{a,b}, and Akua Asa-Awuku^{a,b,*}

^aCollege of Engineering, Center for Environmental Research and Technology, University of California—Riverside, Riverside, California, USA;

^bDepartment of Chemical and Environmental Engineering, University of California—Riverside, Riverside, California, USA

ABSTRACT

Traffic-related pollutants are an ever-growing concern. However, the composition of particle emissions from new vehicle technologies using relevant current and prospective fuel blends is not known. This study tested four current and up-and-coming vehicle technologies with nine fuel blends with various concentrations of ethanol and iso-butanol. Vehicles were driven on both the federal test procedure (FTP) and the unified cycle (UC). Additional tests were conducted under steady-state speed conditions. The vehicle technologies include spray-guided gasoline direct injection (SG-GDI), wall-guided gasoline direct injection (WG-GDI), port-fuel injection flex fuel vehicle (PFI-FFV), and a wall-guided GDI-FFV. The fuels consisted of 10–83% ethanol and 16–55% iso-butanol in gasoline. The composition of soot, water-insoluble mass (WIM), water-soluble organic mass, and water-insoluble organic mass (WIOM), and OM was measured. The majority of emissions over FTP and UC were water-insoluble (>70%), and WIOM contributes mostly to OM. PFIs have lower soot and particulate matter (PM) emissions in comparison to the WG-GDI technology even while increasing the renewable fuel content. SG-GDI technology, which has not penetrated the market, show promise as soot and PM emissions are comparable to PFI vehicles while preserving the GDI fuel economy benefits. The WIM fraction in GDI-FFV consistently increased with increasing ethanol concentration. Lastly, the impact of the future vehicle emissions and traffic pollutants is discussed. SG-GDI technology is found to be a promising sustainable technology to enhance fuel economy and also reduce PM, soot, and WIM emissions.

ARTICLE HISTORY

Received 17 January 2016
Accepted 6 November 2016

EDITOR

Matti Maricq

1. Introduction

Exposure from traffic-related emissions is projected to significantly impact the future US population (Extended Data 2 and Extended Data Table 3 in Leliveild et al. 2015). However, tail-pipe emissions of potential and some current combinations of fuels and vehicle technologies are unknown. Research into light-duty vehicles and fuels has recently expanded due to the Renewable Fuels Standard (RFS) and the revised Corporate Average Fuel Economy Standards (CAFE) (Renewable Fuels Association [RFA] 2007; US Environmental Protection Agency [EPA] 2010). Automotive manufacturers are continuously developing new technologies to reduce emissions and to improve fuel economy to meet the US Federal regulations.

Gasoline direct injection (GDI) vehicle technology has a demonstrated record of enhanced fuel economy compared with the once standard port-fuel injection (PFI) engine. Thus, since 2007, the number of GDI vehicles has rapidly increased in the United States (Zhao et al. 1999; Alkidas 2007; Transportation and Climate Division 2013). By 2025, approximately 93% of the light-duty passenger vehicle market will consist of GDI engines (Transportation and Climate Division 2013). There are two prominent classes of GDI engine architectures: wall-guided (WG) GDI and spray-guided (SG) GDI (Solomon et al. 2000; Drake et al. 2005; Alkidas, 2007). WG-GDI has been tested readily and emit five to six times more particulate matter (PM) than PFI vehicles (Karavalakis et al. 2015a; Alkidas 2007; Maricq et al. 2013). The SG-GDI technology is costly and its

CONTACT Akua Asa-Awuku ✉ akua@engr.ucr.edu 📧 Department of Chemical and Environmental Engineering, University of California—Riverside, 900 University Avenue, Riverside, CA 92521, USA.

*Current affiliation: Department of Chemical and Biomolecular Engineering, University of Maryland, College Park, Maryland, USA

Color versions of one or more of the figures in the article can be found online at www.tandfonline.com/uast.

📎 Supplemental data for this article can be accessed on the [publisher's website](#).

manufacturing and subsequent testing has been limited. Yet, SG-GDI may also potentially improve fuel economy and reduce PM associated with GDI engines (Karavalakis et al. 2015a). However, little is known about the particle composition emitted from newer vehicle technologies such as SG-GDI engines.

In addition, the use of alternative non-petroleum-based ethanol provides diversity from fossil fuel resources and has gained popularity in the automotive industry. Conventional PFI and GDI vehicles are not equipped to consume corrosive higher ethanol concentrations, thus flex fuel vehicles (FFVs) are fitted with materials to withstand up to 85% ethanol (E85). The mainstream use of FFVs has been limited for multiple reasons, mainly (a) the fuel distribution infrastructure (pipelines, underground storage tanks, transportation vehicles, etc.) must be retrofitted to withstand ethanol corrosion, and (b) the ongoing debate on the environmental impact of ethanol use (e.g., enhanced ozone health risk (Jacobson 2007) or reduced ground level ozone (Salvo and Geiger 2014)) has yet to be resolved. Changes in vehicle technology and alcohol fuel content will modify the current and the future traffic-related pollutants, and both must be explored concurrently. Water-soluble organic mass (WSOM) and water-insoluble organic mass (WIOM) fractions could increase with increased alcohol content and changes in vehicle technology. WSOM and WIOM can have severe health implications as well as climate impacts (Verma et al. 2013; Gutiérrez-Castillo et al. 2006; Ervens et al. 2005). Furthermore, the future scenarios of the climate and the health burden of regional traffic pollutants require aerosol composition information.

Recent studies have provided some data on PM speciation of advanced engine technologies for lower (<50%) ethanol blends. Karavalakis et al. (2014a) showed no significant black carbon (BC) trends of GDI vehicles operating on 10–20% ethanol and 16–32% iso-butanol in gasoline. Short et al. (2015a) determined that roughly 30% of PM emissions were WSOM for GDI vehicles tested with both ethanol concentrations of 10 to 20% and iso-butanol concentrations of 16 to 32%. Storey et al. (2014) showed no statistical differences in elemental carbon (EC) between 0% and 30% ethanol in gasoline and 45% iso-butanol in gasoline operating in a GDI engine. In addition, organic carbon (OC) emissions decreased with higher alcohol concentration in a GDI

engine (Storey et al. 2014). Studies of particle composition for fuels with high (>50%) alcohol content in gasoline vehicles are scarce. Only Dutcher et al. (2011) showed that BC emissions decreased by over 50% with increasing ethanol concentration (E0 to E85) for a port-fuel injection flex fuel vehicle (PFI-FFV).

This study investigates the particle composition differences in emissions between WG-GDI, SG-GDI, and FFVs with varying gasoline blends of ethanol and iso-butanol. We explored and compared emissions from engine technologies (PFI, WG-GDI, and SG-GDI) that have dominated and may dominate the market. Furthermore, we investigated the growing use of renewable fuels in these engines. This study extends the previous discussion by Short et al. (2015a) and adds data to the growing body of work of emissions from fuels with more than 50% ethanol content. Notably, it is the first study to provide particle speciation, specifically water-soluble organic carbon (WSOC), water-insoluble mass (WIM), and WSOM from gasoline direct injection flex fuel vehicle (GDI-FFV) and SG-GDI vehicles, two technologies that have the potential to significantly penetrate the future vehicle fleet and modify traffic-related pollutants. It is also noted that Storey et al. (2012) and Parks et al. (2016) have published EC/OC analysis for an SG-GDI vehicle. Soot, WIM fractions, WSOM, WIOM, and OM data are presented. The soot and WIM fractions are measured in real-time during transient and steady-state driving conditions. The WSOM and OM are derived from integrated filter measurements. The WIOM and OM particle analysis are novel and the use of both steady-state and transient cycle data from vehicle emission testing is rare. The coupling of real-time and integrated filter measurements from a relevant forecast of advanced vehicle and fuel technologies provides important information and a critical understanding of different contributions to the traffic-related PM burden for the future regional health burden and global climate scenarios.

2. Experimental

2.1. Test vehicles

The test vehicles and their specifications and mileages are listed in Table 1. The vehicles included two FFVs and two conventional vehicles. Both FFVs were light-duty

Table 1. Test vehicle specifications.

Vehicle make and model year	Engine displacement and configuration	Injection system	Emission control regulations	Mileage
2012 Mercedes Benz E350 (SG-GDI)	3.6 L V6	Spray-guided GDI	LEV II, SULE V	10,996
2012 Mazda 3 (WG-GDI)	2.0 L I4	Wall-guided GDI	LEV II, SULE V	18,851
2013 Ford F150 (PFI-FFV)	3.7 L V6	PFI	LEV II, ULE V	13,687
2014 Chevrolet Silverado (GDI-FFV)	5.3 L V8	GDI	LEV II, ULE V	2,649

pickup trucks. The Ford F150 is equipped with a PFI engine and the Chevrolet Silverado used a WG-GDI engine. The other two vehicles were light-duty passenger cars with different GDI technology engines. The Mazda 3 is equipped with an SG-GDI engine, and the Mercedes-Benz E350 is equipped with a WG-GDI engine. WG-GDI engines have a fuel injector mounted on the side of the combustion chamber that sprays fuel toward the piston bowl surface. All vehicles were certified to low emitting vehicle (LEV) II and ultra low emitting vehicle (ULEV), or super ultra low emitting vehicle (SULEV) emission standards.

2.2. Fuel specifications

All vehicles were tested on the base fuel, E10 (10% ethanol and 90% gasoline). Both SG-GDI and WG-GDI were tested with six custom-blended ethanol and iso-butanol gasoline fuels. This included E15 and E20. In addition, these vehicles were tested on blends of 16, 24, and 32% by volume of iso-butanol respectively (denoted as B16, B24, and B32). B16 is the oxygenated equivalent of E10. The PFI-FFV and GDI-FFV were tested on four custom-blended ethanol and iso-butanol fuels (including E10). The other two higher ethanol fuels include E51 and E83. The higher iso-butanol-blended fuel was 55% iso-butanol fuel (B55). These fuels were custom-made to control Reid vapor pressure (RVP), oxygen content, and fuel volatility among other properties. Specific fuel properties can be found in the Table S1 (available in the online supplementary information [SI]).

2.3. Experimental protocol

Vehicles were tested at CE-CERT's Vehicle Emissions Research Laboratory (VERL). VERL is equipped with a Burke E. Porter 48" barrel light-duty chassis dynamometer. The facility is also equipped with a constant volume sampler (CVS) for emissions' sampling. All vehicles were tested on both the federal test procedure (FTP) and the unified cycle (UC). In addition, each vehicle (with the exception of Chevrolet Silverado) was tested over three steady-state speeds of 30, 50, and 70 miles per hour (mph). Each cycle was performed in triplicate for the study with the average of three tests being reported and the standard deviation (SD) being the error bar. Data are not reported for days of instrument malfunction and data recording errors.

The FTP and UC, respectively, consist of three different types of driving simulations or phases. A speed versus time trace for each is shown in Figure S1 (available in the online supplementary material). Phase 1 is the "cold start" phase. The vehicle's engine and catalyst are cooled

for at least 8 h before phase 1, simulating daily initial starting conditions. Phase 2 is the stabilized phase; the vehicle's engine and catalyst are warm; so driving conditions represent normal driving after the vehicle is warmed up. After phase 2, the vehicle is turned off for exactly 10 min during the "hot soak" period. Phase 3 proceeds directly after the "hot soak." Phase 3 is a "hot start" phase where driving conditions are identical to phase 1; however, the vehicle now has a warm engine and catalyst. Phase 3 is known to emit fewer emissions compared to phase 1. After an FTP or UC, the steady-state testing of the vehicle was performed. Each steady-state speed is run for exactly 10 min after a warm-up period, and after the operation was stabilized.

2.4. Particulate matter measurements and analysis

The overall study included particle and gaseous measurements (Figure S2). The focus of this article is particle physical and chemical compositions. Figure S2 shows the inlet connections of the instruments, the instrument flow rates, and the experimental setup. The measurements for this article include gravimetric filter-based particle measurements and real-time particle measurements. The total PM results were measured gravimetrically with the particles collected on Teflon filters. The individual total PM results are found in Figure S5 and in Karavalakis et al. (2014b). The following describes the particle instrumentation and analysis used in this article.

Organic Mass was measured for both Ford F150 and Chevrolet Silverado (FFVs) over the FTP cycle. Quartz filters were used for this analysis and the OM concentration was reported for the particle over all particle diameters. The OC was measured using a Sunset Laboratory Elemental Carbon (EC)/OC Lab analyzer, utilizing the National Institutes of Safety and Health (NIOSH) 5040 protocol. The OC was collected using one quartz filter at ambient temperature with a filter face velocity of 60 lpm. The measurement was a thermal-optical method; the sample was desorbed thermally from the filter with helium gas and oxidized as heat increased. The sample was analyzed using a flame ionization detector (FID). Values of OC were multiplied by a factor of 1.55 to take into account the non-carbonaceous organic matter, giving the OM value (Turpin and Lim 2001; Cheung et al. 2009).

For each transient test, Teflon filters were sampled to quantify WSOC and WSOM. WSOC or WSOM was determined for the whole particle over all particle diameters. Particles were first extracted from Teflon filter into an aqueous solution. Filters were placed in a clean 60-mL amber vial and 60 mL of Millipore® water (TOC ~70 ppb) was added. Vials were then sonicated for

approximately 90 min at room temperature. After sonication, the sample was removed with a Whatman® 25-mm syringe filter (to extract any large water-insoluble materials). A pendant drop tensiometer (Attension Theta 200, Bioscientific, Stockholm, Sweden) was used for surface tension analysis. The WSOC analysis was performed with a GE Seivers 900 TOC analyzer (GE Sievers, Boulder, CO, USA). The WSOC concentration is multiplied by a factor of 1.6 to convert to WSOM (Turpin and Lim 2001). This factor accounts for all measured water-soluble non-carbonaceous OM. The water-insoluble organic carbon (WIOC) is the WSOC subtracted from OC values. This value was multiplied by 1.4, which accounts for all water-insoluble non-carbonaceous mass, to give the WIOM value. The balance of OM was calculated and the addition of WIOM and WSOM agrees well with total OM values (Figure S3, slope = 0.954, $R^2 = 0.989$). The use of ambient empirical factor in this procedure is consistent with Cheung et al. (2009), who measured fresh tailpipe PM from PFI vehicle and ethanol blends.

The WIM fraction was estimated using a technique described in Short et al. (2014). The method exploits differences in real-time size distributions for particle diameters below 40 nm, i.e., sizes below which insoluble chemistry greatly impacts droplet growth in particle counters. Briefly described here, the size distributions were measured using a scanning mobility particle sizer (SMPS), which consists of an electrostatic classifier (TSI 3080; TSI Inc., Shoreview, MN, USA) used in tandem with a butanol condensation particle counter (B-CPC; TSI 3772) and a water condensation particle counter (W-CPC; TSI 3785). The CPCs use a different working fluid of either water or butanol. Two distinct particle concentrations from B-CPC and W-CPC were measured for each particle diameter. The differences between the two particle concentrations determined the WIM fraction. The particle concentrations for each particle diameter selected during the sampling period (i.e., cycle phase or overall cycle) was summed over each cycle or phase. This method was performed for both W-CPC and B-CPC measurements; the ratio of W-CPC to B-CPC gave an overall ratio of the difference in W-CPC to B-CPC particle counts. This ratio determines an overall hygroscopicity value, κ , and the overall WIM fraction (Short et al. 2014, 2015a).

Soot concentrations were measured in real-time using the AVL micro soot sensor (MSS; AVL MSS, Plymouth, MI, USA). The AVL MSS measures the soot concentration based on the whole particle, or over all particle diameter sizes from particle stream (Schindler et al. 2004). The MSS is a photoacoustic instrument that has a lower detection limit of $5 \mu\text{g m}^{-3}$. An infrared (IR) light beam of 808 nm was directed at the particle stream. Once the light beam

was absorbed by the soot particles, sound waves were produced and measured using a microphone. The GDI vehicle's emission streams were diluted by 5 to 1 for soot emission measurements to keep the analyzer from over ranging since the emissions were higher than those of the PFI vehicle.

3. Results and discussion

The data collected and analyzed in this study were extensive. For brevity, we focused on the particle composition as it may pertain to health and the climate future scenarios of traffic pollutants. As such, additional data and figures relevant to vehicle testing and emissions could be found in companion articles and supplemental material. Specifically, each subsequent section will discuss emission factors (EFs) of individual compositions and the contribution of each component to overall PM mass. As mentioned above, error analysis shown is the average and SD of three experimental trials. In the case of insufficient data (Table S2), error bars were nonexistent and only one trial or no trials were reported. Single trials provided insight into the overall water-soluble/insoluble fractional changes of various fuel and vehicle tests, and are included in the discussion.

3.1. Soot emission factors

The soot EFs were measured in real-time using the MSS instrument over both UC and FTP cycles. The soot fraction (concentration divided by the total PM mass) is discussed in Section 3.6. Figure 1 shows the soot EFs over both FTP and UC for all four vehicles tested. WG-GDI and GDI-FFV vehicles emitted six and eight times, respectively, more soot compared with the tested SG-GDI and PFI-FFV (Figure 1). SG-GDI emitted similar amounts of soot as the PFI engine. The WG-GDI technology can potentially reach similar levels if alcohol content is significantly increased. Both WG-GDI and GDI-FFV showed significant decrease in soot emission factors with increased ethanol concentration. The EFs of WG-GDI vehicle decreased 81% over FTP and 83% over UC as ethanol increased in E10 to E20 fuel blends. The GDI-FFV showed a 93% decrease in soot EFs from E10 to E83 fuel blends over FTP, and a 71% decrease from E10 to E51 fuel blend over UC.

Vehicle technology and fuels impact soot emissions, thus affecting the total amount of BC or soot emitted. FFVs are likely to produce less soot with higher alcohol fuels; and increasing the alcohol content in GDI-FFV and PFI-FFV decreases the soot EF by up to 90%. Increased ethanol concentrations reduce soot emissions for FFVs and GDI vehicles.

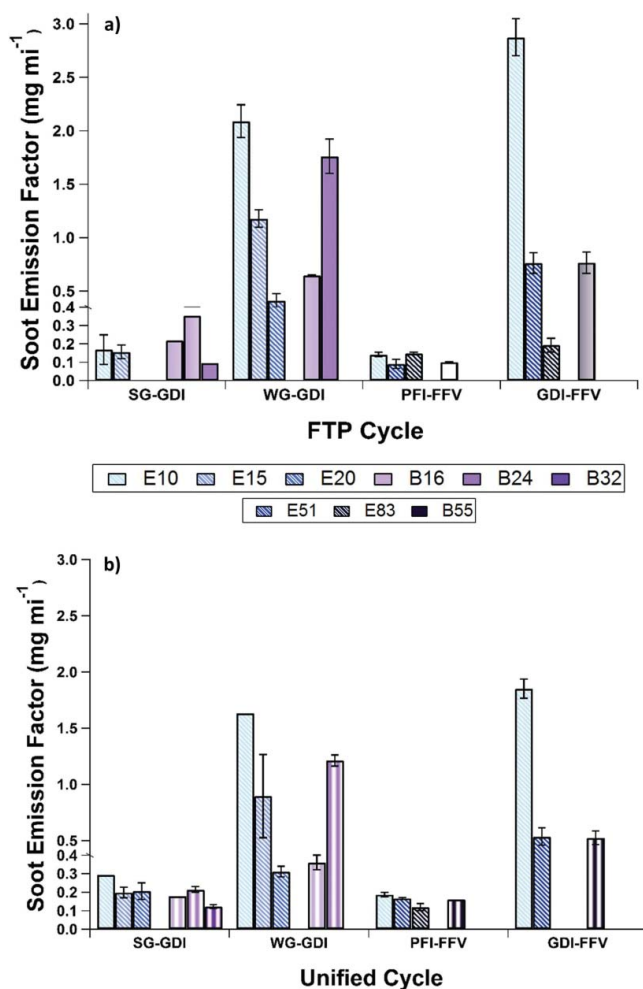


Figure 1. The soot emission factor over both (a) FTP and (b) unified cycles for WG-GDI, SG-GDI, PFI-FFV, and GDI-FFV.

3.2. WSOM emission factors

The WSOM data were collected cumulatively on filters over UC and FTP (Figure 2). Again, error bars of WSOM EFs (Figure 2) were shown only if three trials were conducted and all required measurements were available for analysis (see Table S2 for detailed information on the number of trials used to determine error bars). In addition, some fuel data were not reported and have been noted in Figure 2. The majority of WSOM EFs are below 1 mg/mi for all four vehicles over both cycles. WSOM emissions were variable across the study. For example, during the FTP cycle, increasing the alcohol content increased the WSOM EFs for WG-GDI and PFI-FFV vehicles (Figure 2). For UC, the WSOM EFs remained relatively constant with increasing alcohol content, suggesting that for a more aggressive and higher speed cycle, WSOM EFs were insensitive to alcohol content. The PFI-FFV showed a 150% increase in the WSOM EF with increased ethanol content from E10 to E83 fuels over the FTP cycle and constant WSOM EFs at

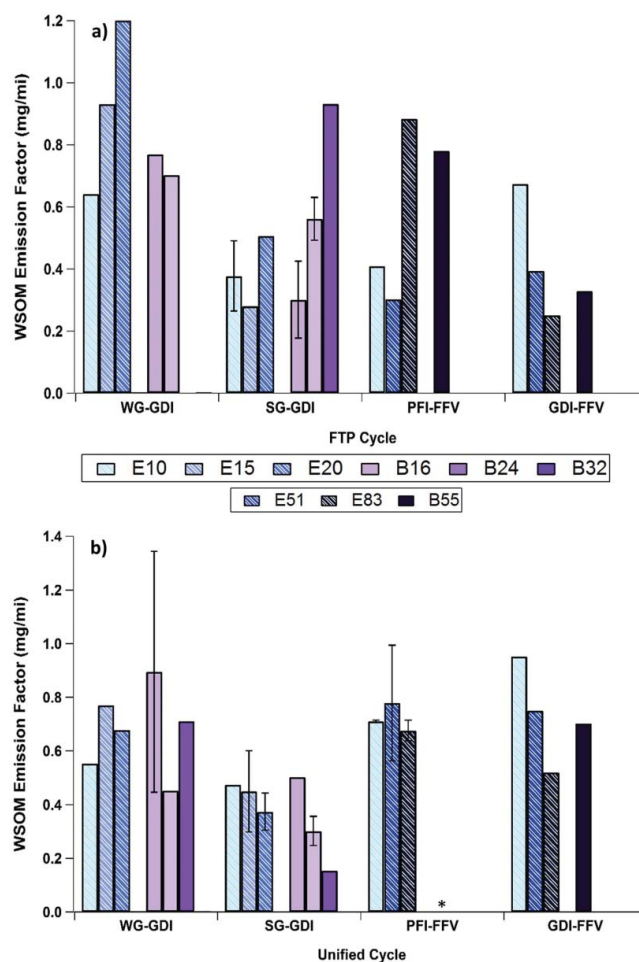


Figure 2. The WSOM emission factors over both (a) FTP and (b) unified cycles for WG-GDI, SG-GDI, PFI-FFV, and GDI-FFV. *Data not available.

0.8 mg/mi for the same fuels over the UC. WG-GDI vehicle showed a 100% increase in the WSOM EF from E10 to E20 fuels over the FTP cycle. The SG-GDI showed a small increase in the WSOM EF with increased ethanol concentration but a 185% increase from B16 to B32 fuels. In addition, a 67% decrease in the WSOM EFs was observed from B16 to B32 fuels over the UC for SG-GDI. Alternatively, the GDI-FFV over the FTP showed the opposite trend. The WSOM EF decreased 63% with increasing ethanol content from E10 to E83 fuels over the FTP and decreased 40% over the UC.

3.3. Estimated WIM fraction for all cycles and by phase

The WIM fractions were estimated over both cycles for all four vehicles, and were consistent. The overall cumulative WIM fractions for WG-GDI, SG-GDI, PFI-FFV, and GDI-FFV are shown in Figure 3. Generally, the WIM fractions are high (>0.6) for all

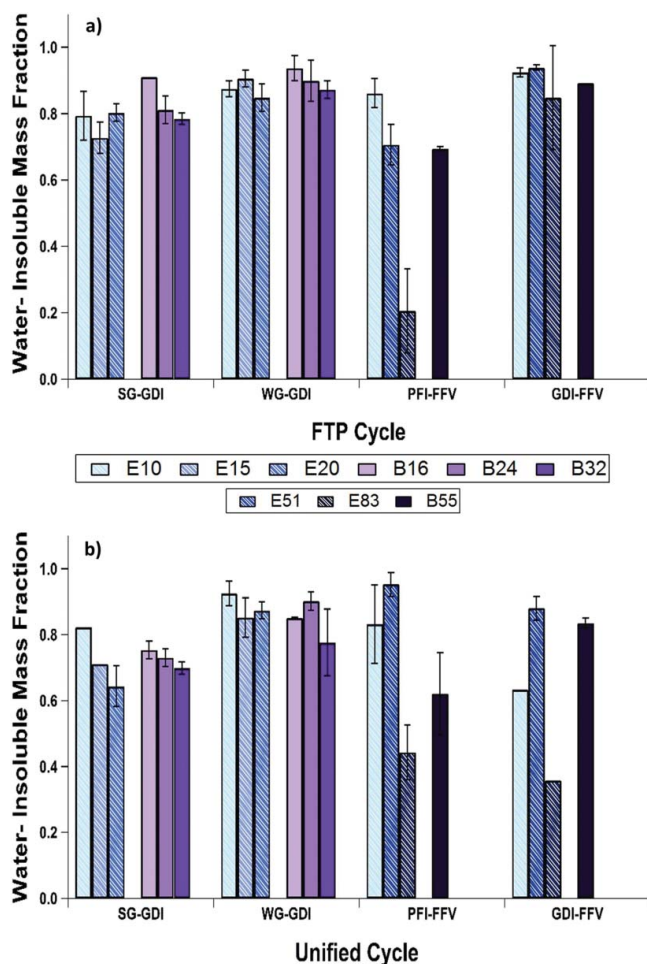


Figure 3. The estimated water-insoluble mass fraction over both (a) FTP and (b) unified cycles for WG-GDI, SG-GDI, PFI-FFV, and GDI-FFV.

vehicles and fuels over both cycles. Light duty passenger cars (SG-GDI and WG-GDI) consistently emitted WIM fractions (>0.75). The amount of WIM emitted by FFVs depended on PFI and GDI engine technology. The GDI-FFV had WIM fractions above 0.8 for all fuels over the FTP cycle. The PFI-FFV shows a wider range in WIM fractions, with low overall WIM fractions for some fuels over both cycles. The GDI-FFV and PFI-FFV have relatively equivalent WIM fraction trends over the UC.

The PFI-FFV showed decreasing WIM fractions with increasing alcohol content over both cycles. Specifically, the PFI-FFV emitted large amount of water-insoluble particle emissions with E10 fuel but low amount of water-insoluble particle emissions with E83 fuel. The decrease from E10 to E83 fuel was 75% for FTP cycle and 50% for UC. The GDI-FFV showed mostly water-insoluble emissions over FTP cycle. Singular data points suggest that over the UC, the WIM fraction decreased 33% over E10 and E83 fuel blends. The E51 and B55 fuel blend WIM fractions (~ 0.85)

were significantly higher compared with the other WIM fractions.

The observed overall WIM fractions can be attributed to changes during separate phases of the cycle. Figure 4 shows WIM fractions for each phase of FTP and UC for SG-GDI, PFI-FFV, and GDI-FFV vehicles. The WG-GDI vehicle WIM data by phase is shown in Figure S4. The SG-GDI and WG-GDI vehicles showed consistent WIM fractions between all three phases for both cycles (some variability existed for SG-GDI with some fuel blends). The FFVs showed more variable WIM fractions between the three phases over both cycles. The E10 and E51 fuel blends had higher WIM fractions between both vehicles and cycles.

The SG-GDI and WG-GDI vehicles had mostly water-insoluble particle emissions by phase consistent with an overall high WIM fraction over the cycle. WG-GDI vehicle emitted very hygroscopic particles over all three phases in both cycles. The SG-GDI shows low WIM fractions for E10 fuel over the phase 2 of FTP cycle, but E20 fuel has a high WIM fraction. Thus, the increase in ethanol content in the fuel increased the WIM fraction for phase 2 of FTP for the SG-GDI vehicle. The iso-butanol fuel blends show a large decrease in the WIM fraction, 48% for FTP, and 67% for UC, with increasing iso-butanol concentration over both cycles for the SG-GDI. Generally, increasing iso-butanol fuels decreased WIM over both cycles, but these decreases are roughly 20% or just above the method uncertainty of 15% (Short et al. 2014).

The FFVs had large decreases in the WIM fraction with higher alcohol content. For the PFI-FFV, large WIM fraction decreases were found with higher alcohol content over FTP cycle for all three phases. Phase 1 had a 76% decrease, phase 2 had a 56% decrease, and phase 3 had a 50% decrease in WIM fraction from E10 to E83 fuel blend. UC also showed large decreases from E10 to E83 fuel blend, but only for phases 1 and 3, which showed decrease of 63% and 43%, respectively. For GDI-FFV, the ethanol fuel blends had similar WIM fractions over the FTP cycle. The B55 fuel blend had fractions that were lower than the E10 fuel blend for all three phases, with a minimum WIM fraction of 0.6 (phase 2). UC decreased WIM fractions, from E10 to E83 fuel blends, by 61% (phase 1) and 54% (phase 3). Phase 2 showed a 243% increase in the WIM fraction from E10 to E83 fuel blends. WIM fractions are sensitive to changes in cycle phase.

3.4. Steady-state κ values and soot concentration

The SG-GDI, WG-GDI, and PFI-FFV vehicles were run for 10 min over each of the three steady-state speeds.

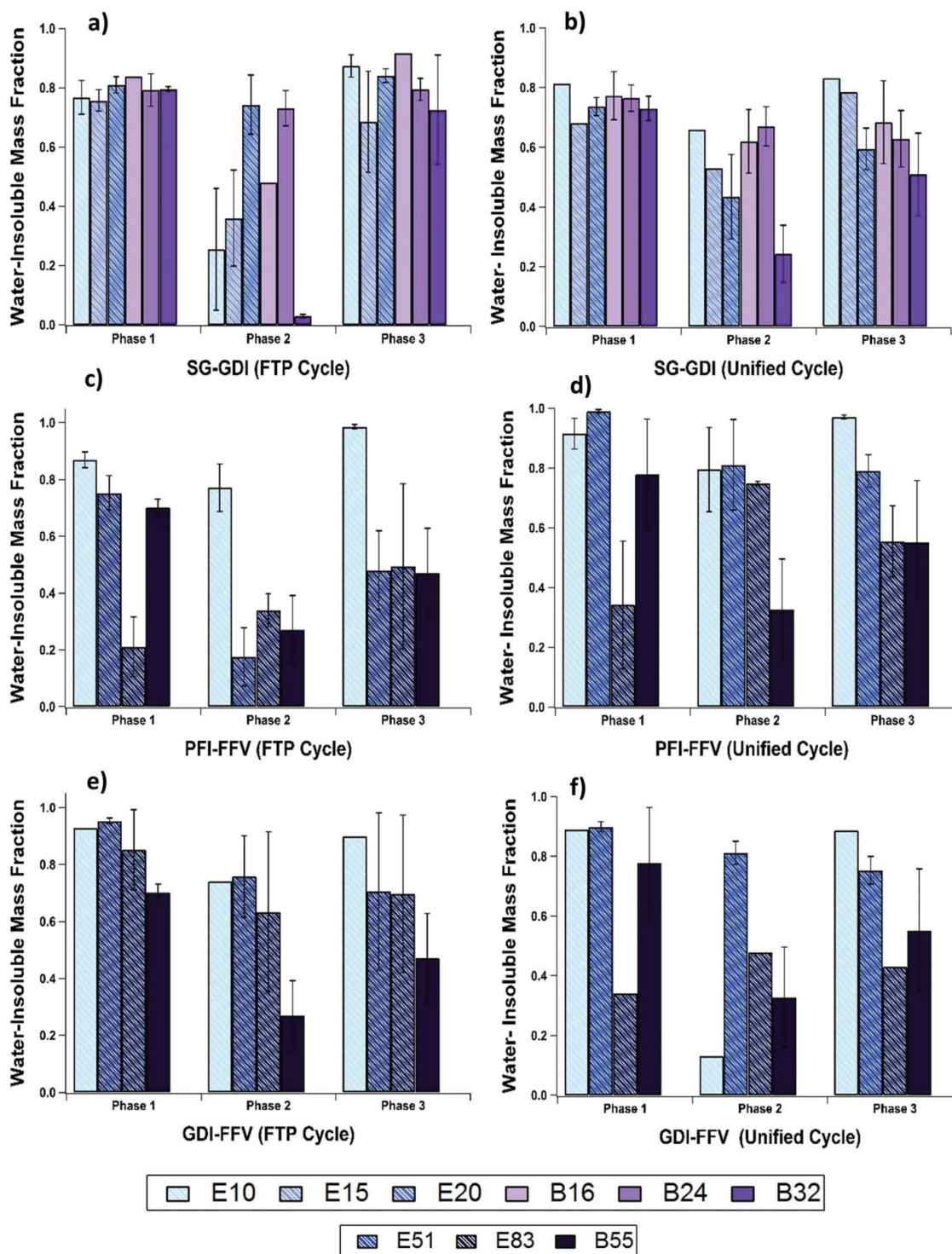


Figure 4. The estimated water-insoluble mass fraction over both cycles for SG-GDI ((a) FTP and (b) UC), PFI-FFV ((c) FTP and (d) UC), and GDI-FFV ((e) FTP and (f) UC). The WG-GDI results are shown in Figure S4.

The κ values and soot concentration averages for each speed and fuel are reported in Figure 5. All three vehicles show a κ value similar to the κ value for sulfuric acid ($\kappa = 0.9$). The κ are shown here to illustrate how the particle hygroscopicity changes with vehicle speed. The κ values were reported during the steady-state speeds instead of WIM fractions because as κ

values approach 1 or become greater than the κ value of sulfuric acid ($\kappa = 0.9$), the calculated WIM fractions become negative. In these cases, κ value provides a clearer understanding of the likelihood of particle water-insolubility. If the particle hygroscopicity is high then the particles are more water-soluble. The opposite is accurate for low particle hygroscopicity values. The

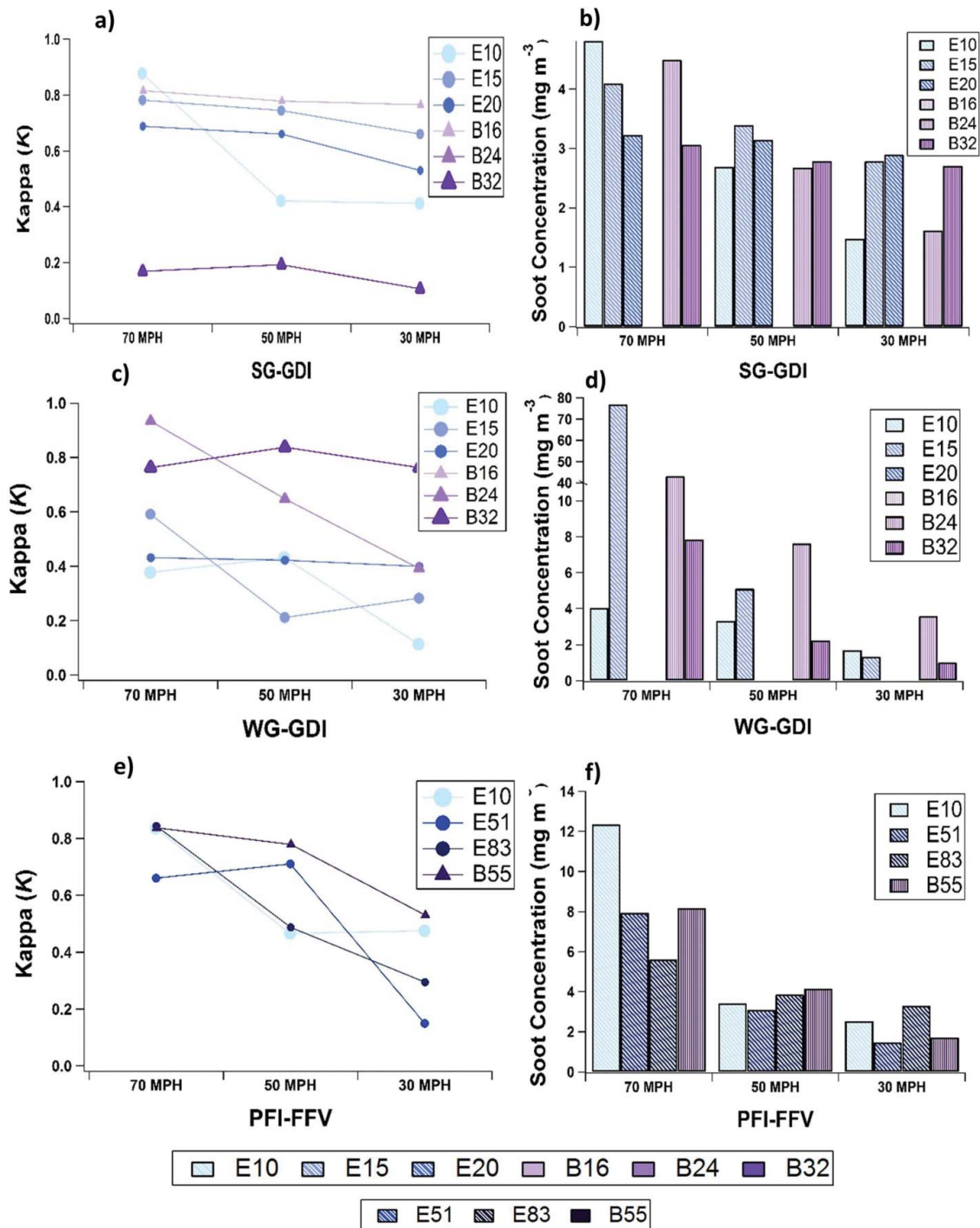


Figure 5. The estimated water-insoluble mass fraction over 70-, 50-, and 30-mph steady-state speeds for SG-GDI ((a) κ and (b) soot), WG-GDI ((c) κ and (d) soot), and PFI-FFV ((e) κ and (f) soot).

SG-GDI vehicle shows κ values that were above 0.5, or were more hygroscopic (with a lone exception of B32 fuel, where the κ value was ~ 0.2). Whereas the WG-GDI vehicle has high κ values, or very hygroscopic particles for 70-mph speed, at 30-mph speed the κ values are low, or the particles are less hygroscopic (except for E20 and B32 fuels, which remained at κ values of ~ 0.42 and ~ 0.80 , respectively).

In general, the higher vehicle speed increased κ values or the particle hygroscopicity. More specifically, the PFI-FFV had a high κ value for 70-mph speed, but at 30-mph speed for E51 and E83 fuel blends, the particles become less hygroscopic, with values of 0.18 and 0.38 respectively. The κ values for the B32 fuel blend for the SG-GDI were low for all three speeds, but for the B32 fuel blend for the WG-GDI, the particles κ value was

high for all three speeds. In addition, soot concentration decreased with decreasing vehicle speed for all three vehicles. The WG-GDI vehicle emitted the highest soot concentration for all three vehicles at 87 mg m^{-3} . Steady-state hygroscopicity and soot results were not realistic of real-world driving conditions; however, their agreement in trends provides key information about particle composition.

3.5. Water-soluble and insoluble organic contributions to OM

The calculation of WIOM and OM EFs are described in Section 2.3. The PM EFs are shown in Figure S4. The EFs of WSOM, WIOM, and PM mass are shown in Figure 6a for FFVs over FTP. Like WSOM, WIOM EFs are variable and do not exhibit strong fuel trends. FFVs on E51 emit the most WIOM. The WSOM EFs increased

with increasing ethanol content for PFI-FFV and decreased with increasing ethanol content for GDI-FFV (Section 3.2). For reference, the EC and OC EFs for GDI-FFV are published in Karavalakis et al. (2014c) with total EC+OC fractions of the total gravimetric PM being 0.76 for E10, 0.73 for E51, 0.58 for E83, and 0.49 for B55. In addition, the PFI-FFV showed total EC+OC fractions of the total gravimetric PM values of 0.26 for E10, 0.63 for E51, 0.24 for E83, and 0.25 for B55.

The WIOM and WSOM fractions of the total PM mass over the FTP cycle are shown in Figure 6b. The WSOM/PM mass fractions for PFI-FFV are much larger (>40%) compared with the GDI-FFV (<14%). In addition, the GDI-FFV showed that increased alcohol concentrations increased the WIOM/PM mass fractions. The combined WIOM and WSOM (or OM) fractions ranged from about 43 to 72% of the total PM mass for PFI-FFV, as shown in Figure 2b. Due to the increase in

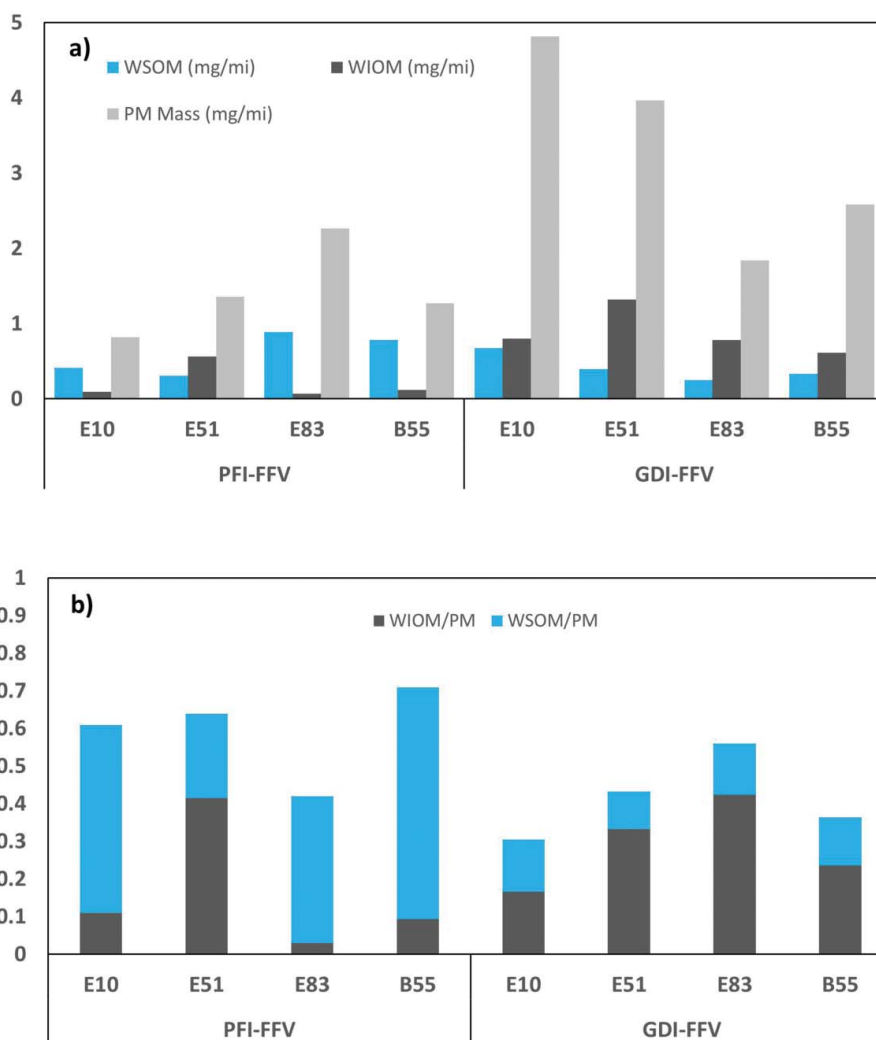


Figure 6. The WSOM, WIOM, and PM mass emission factors for both (a) PFI-FFV and GDI-FFV (b). The WSOM and WIOM PM mass fractions in a stacked bar graph over FTP cycle for PFI-FFV and GDI-FFV. The addition of both WSOM and WIOM represent the OM/PM mass fraction.

the PM mass emissions, the fraction of WIOM and WSOM decreased for E83 for PFI-FFV. The PFI-FFV shows that the majority of OM emissions for E10 and E83 fuels were WSOM, and the WSOM/PM mass fraction ranged from 0.48 to 0.37 from E10 to E83 fuels. The B55 blend showed the highest WSOM emissions for PFI-FFV, which was 60% of the total PM. For GDI-FFV, the WIOM PM mass fractions increased with increasing ethanol concentration from 0.18 for E10 fuel to 0.42 for E83 fuel. Note that the increase in WIOM fractions are due in part to the decrease in total PM mass for GDI-FFV with increasing ethanol content. The WSOM fraction for GDI-FFV was constant (~ 0.14).

Figure 6b shows the combination of WSOM and WIOM in relationship to the total PM mass (the sum of WSOM and WIOM equals to the total OM of particles). Effectively, Figure 2b shows the OM/PM mass fractions for FFVs over the FTP cycle. The OM/PM mass fraction varies greatly for PFI-FFV, but there is a consistent fuel trend of increasing OM/PM mass fractions with increased ethanol content for GDI-FFV. As stated above, the WIOM/PM mass also increases with increased ethanol content. Both trends for GDI-FFV are attributed more to the decreasing total PM mass with increasing alcohol content than changes with the particle composition. The differences in OM/PM mass trends between the vehicles might be attributed to the differences in their engine technologies rather than the increased ethanol content. Specifically, the fuel injecting into the piston cylinder of GDI vehicles is not as well mixed as that for PFI vehicles; the oxygen in the higher alcohol appears to have a larger impact in reducing PM in rich zones of GDI vehicles than during the combustion of PFI (Drake et al. 2005; Alkidas 2007).

3.6. Soot/PM fraction

The total amount of soot for both FTP and UC and all four vehicles was divided by the total amount of PM mass (Figure 7). The total PM mass emission factors were measured gravimetrically with particles collected on a teflon filter, and are reported in the companion articles to this study (Karavalakis et al. 2014b, 2015). The soot/PM mass EFs show that for the WG-GDI vehicle, on E10 fuel, $\sim 75\%$ of the PM emissions were soot over the FTP cycle. The fraction for all four vehicles range from 0 to 1, and is highly variable. On average, SG-GDI and WG-GDI vehicles have large soot/PM mass fractions compared with the FFV vehicles for both FTP and UC. In addition, increased alcohol concentration in the fuel decreases the soot/PM mass fraction over both cycles. A 60% and 37% decrease in the soot/PM mass fraction was reported from E10 to E15 fuel blend for the SG-GDI vehicle over FTP and UC respectively. For WG-GDI vehicle, a 59% and 47% decrease in the soot/PM mass fraction is shown from E10 to E20 fuel blend over FTP and UC respectively. For PFI-FFV and GDI-FFV vehicles, a 68% and 75% decrease in the soot/PM mass fraction, respectively, was shown from E10 to E83 fuel blends over FTP. Over UC, the FFVs tested did not show a difference in soot/PM mass fraction with increasing ethanol concentration. The soot fractions for WG-GDI vehicles are $\sim 75\%$ of PM emissions, and were equivalent to the values reported by Maricq et al. (2013).

There is a good correlation between soot/PM mass emissions and WIM fractions, given that the overall cumulative WIM fractions only represent particle water insolubility below 40 nm and not bulk composition. The cumulative WIM fractions also showed a similar trend

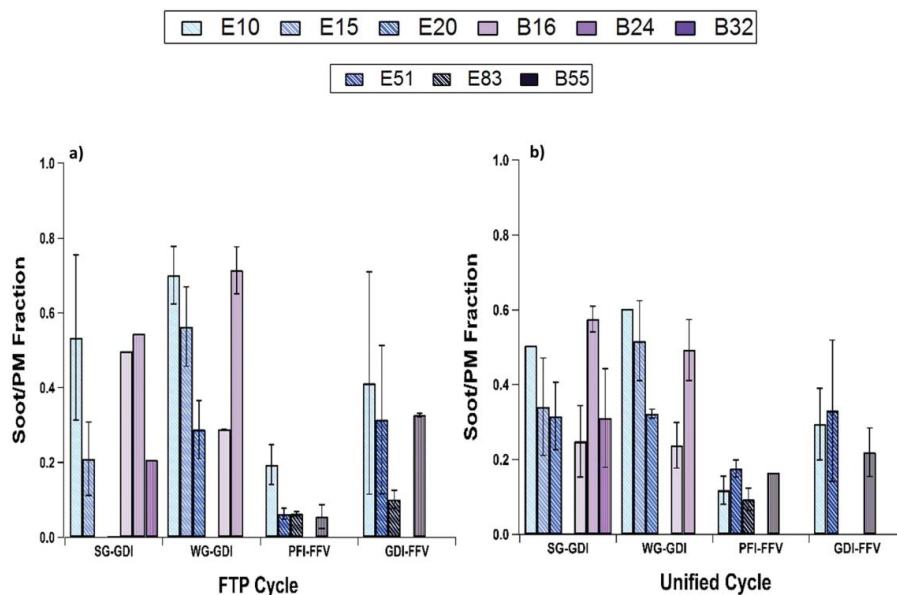


Figure 7. The soot/PM mass fraction over both (a) FTP and (b) unified cycles for WG-GDI, SG-GDI, PFI-FFV, and GDI-FFV.

with soot/PM mass fraction. The addition of soot and WIOM contributions to the total PM mass showed a fraction estimate that was similar to, but below, those of WIM fraction. It is important to note that OM and soot emissions are determined for all particle diameters and bulk composition, whereas WIM fractions are for particle diameters below 40 nm, which contribute small discrepancy in estimates.

4. Summary and implications

The composition of aerosol pollutants is as important as its abundance. WSOM, WIOM, WIM, and soot/BC are significant components of total PM mass, making up the majority (~70–100%) of the total PM mass depending on the vehicle technology and fuel. Soot and WIM dominate the fraction of freshly emitted aerosol across all fuels and vehicle technologies. The contributions of WIM, WIOM, WSOM, and OM are known to have adverse health effects. The future emission studies should examine particle composition more closely by reporting not only the WSOM/WIOM and soot fractions but also the ionic components of PM to determine the overall mass balance of PM emissions from a variety of vehicles and fuels.

Furthermore, if the United States is to continue the use of prevalent engine technologies (PFI and WG-GDIs) with higher alcohol fuel contents in FFVs, we can expect emissions with significant insoluble contributions. For the GDI-FFV, the WSOM/PM mass and WIM fractions correlate well; low WSOM fractions (<15%) were measured with high WIM fractions (>75%). The PFI-FFV had much larger WSOM/PM mass fractions than the GDI-FFV, while the GDI-FFV had larger WIOM/PM mass emissions. All vehicles had high κ values (>0.75); however, only the PFI-FFV decreased WIM fractions with increased alcohol content.

Insoluble fractions are modified during separate phases of transient cycle testing. Results indicate that vehicle speed strongly correlates with the particle hygroscopicity value; increased vehicle speed increased the apparent hygroscopicity and decreased the amount of soot and water-insoluble particles. Thus, the hygroscopicity of particle pollutants was not dominated by engine technology or fuel and reinforced the findings of previous studies (Short et al. 2015a,b). Unfortunately, steady-state emission tests are not realistic of real-world driving conditions and are rarely presented in literature. However, these additional tests, in conjunction with transient cycles, provide additional information that elucidates the impact of aggressive driving cycles and the source of insoluble particles. Vehicle speed clearly has an effect on particle water solubility that should be considered when defining regional regulations. Soluble particle emissions are likely

prevalent near major roadways where increased speeds of 70 mph prevail. Communities near these roadways could be particularly vulnerable to water-soluble particle composition, possibly impacting residents' overall health.

In the future climate emission scenarios, the RFS mandates to increase ethanol usage in gasoline must be included, as emissions may result in a reduction in soot and BC (short-lived climate forcers). A combination of SG-GDI technology and higher ethanol concentration could provide significant reductions in overall PM, and reduce both BC and OM emissions from light-duty vehicles while providing increased fuel efficiency. Conversely, increased use of WG-GDI and GDI-FFV technologies could increase the overall BC emission inventory from light duty vehicles. Only higher ethanol concentrations (E83) in GDI-FFV showed potential for large reductions in the overall emitted BC. The contributions of OM, WSOM, and WIOM might not have a notable impact on climate as BC but may have larger implications for human health. Thus, all technologies and fuels tested have various advantages and disadvantages for regional air quality and global climate.

Of the vehicle technologies tested in this study, results here suggest that SG-GDI light-duty cars are promising environmentally sustainable vehicles with high fuel economy to be used with renewable fuels to mitigate particle emissions. Yet, SG-GDI is the most costly to manufacture and the least characterized technology. As such, the critical data and results presented here contribute to the dearth of literature and highlight the need for additional vehicle testing necessary to study the abundance and composition of particle emissions of new technologies and their subsequent impacts.

Acknowledgments

The authors would like to thank Mark Villela and Kurt Bumiller for their technical support for this study.

Funding

This work was supported by the University of California Transportation Center and the US Environmental Protection Agency (EPA) grant number 83504001. The contents of this article are solely the responsibility of the grantee and do not necessarily represent the official views of the EPA. Further, the EPA does not endorse the purchase of any commercial products or services mentioned in the publication. Diep Vu thanks the EPA for the STAR Fellowship Assistance, Agreement No. FP-91751101.

References

- Alkidas, A. C. (2007). Combustion Advancements in Gasoline Engines. *Energy Conv. Manage.*,48(11):2751–2761.

- Cheung, K., Polidori, A., Nyziachristos, L., Tzamkiozis, T., Samaras, Z., Cassee, F., Gerlofs, M., and Sioutas, C. (2009). Chemical Characteristics and Oxidative Potential of Particulate Matter Emissions from Gasoline, Diesel, and Biodiesel Cars. *Environ. Sci. Technol.*, 2009(43):6334–6340.
- Drake, M. C., Fansler, T. D., and Lippert, A. M. (2005). Stratified-Charge Combustion: Modeling and Imaging of a Spray-Guided Direct-Injection Spark-Ignition Engine. *Proc. Combust. Inst.*, 30(2):2683–2691.
- Dutcher, D. D., Stolzenburg, M. R., Thompson, S. L., Medrano, J. M., Gross, D. S., Kittelson, D. B., and McMurry, P. H. (2011). Emissions from Ethanol-Gasoline Blends: A Single Particle Perspective. *Atmosphere*, 2:182–200; doi:10.3390/atmos2020182.
- US Environmental Protection Agency (EPA). (2010, April). *EPA and NHTSA Finalize Historic National Program to Reduce Greenhouse Gases and Improve Fuel Economy for Cars and Trucks*. EPA Report EPA-420-F-10-014, US EPA Office of Transportation and Air Quality, Washington DC.
- Ervens, B., Feingold, G., and Kreidenweis, S. M. (2005). Influence of Water-Soluble Organic Carbon on Cloud Drop Number Concentration. *J. Geophys. Res.*, 110:D18211.
- Gutiérrez-Castillo, M., Roubicek, D. A., Cebrián-García, M. E., De Vizcaya-Ruiz, A., Sordo-Cedeño, M., and Ostrosky-Wegman, P. (2006). Effect of Chemical Composition on the Induction of DNA Damage by Urban Airborne Particulate Matter. *Environ. Mol. Mutagenesis*, 47:199–211.
- Jacobson, M. Z. (2007). Effects of Ethanol (E85) Versus Gasoline Vehicles on Cancer and Mortality in the United States. *Environ. Sci. Technol.*, 41(3):4150–4157.
- Karavalakis, G., Short, D., Vu, D., Villela, M., Asa-Awuku, A., and Durbin, T. (2014a). Evaluating the Regulated Emissions, Air Toxics, Ultrafine Particles, and Black Carbon from SI-PFI and SI-DI Vehicles Operating on Different Ethanol and Iso-Butanol Blends. *Fuel*, 128:410–421.
- Karavalakis, G., Short, D., Russel, R., Jung, H., Johnson, K. C., Asa-Awuku, A., and Durbin, T. D. (2014b). Assessing the Impacts of Ethanol and Iso-Butanol on Gaseous and Particulate Emissions from Flexible Fuel Vehicles. *Environ. Sci. Technol.*, 48(23):14016–14024.
- Karavalakis, G., Short, D., Chen, V., Espinoza, C., Berte, T., Durbin, T., Asa-Awuku, A., Jung, H., Ntziachristos, L., Amanatidis, S., and Bergmann, A. (2014c). Evaluating Particulate Emissions from a Flexible Fuel Vehicle with Direct Injection when Operated on Ethanol and Iso-butanol Blends. *SAE Technical Paper 2014-01-2768*.
- Karavalakis, G., Short, D., Vu, D., Russell, R., Asa-Awuku, A., Jung, H., Johnson, K., and Durbin, T. (2015). The Impact of Ethanol and Iso-Butanol Blends on Gaseous and Particulate Emissions from Two Passenger Cars Equipped with Spray-Guided and Wall-Guided Direct Injection SI (Spark Ignition) Engines. *Energy*, 82:168–179.
- Lelieveld, J., Evans, J. S., Fnais, M., Giannadaki, D., and Pozzer, A. (2015). The Contribution of Outdoor Air Pollution Sources to Premature Mortality on a Global Scale. *Nature*, 525:367–371.
- Maricq, M. M., Szente, J. J., Adams, J., Tennon, P., and Tumpsa, T. (2013). Influence of Mileage Accumulation on the Particle Mass and Number Emissions of Two Gasoline Direct Injection Vehicles. *Environ. Sci. Technol.*, 47(20):11890–11896, doi:10.1021/es402686z.
- Parks, J., Storey, J., Prikhodko, V., and Debusk, M. (2016). Filter-Based Control of Particulate Matter from a Lean Gasoline Direct Injection Engine. *SAE Technical Paper 2016-01-0937*.
- Renewable Fuels Association (RFA). (2007). *Federal Regulations: Renewable Fuels Standard*. RFA, Washington DC.
- Salvo, A., and Geiger, F. M. (2014). Reduction in Local Ozone Levels in Urban Sao Paulo Due to a Shift From Ethanol to Gasoline Use. *Nature Geosci.* 7:450–458. doi:10.1038/ngeo2144.
- Schindler, W., Haisch, C., Back, H. A., Niessner, R., Jacob, E., and Rothe, D. (2004). A Photoacoustic Sensor System for Time Resolved Quantification of Diesel Soot Emissions. *SAE Technical Paper 2004-01-0968*.
- Short, D., Giordano, M., Zhu, Y., Fine, P., Polidori, A., and Asa-Awuku, A. (2014). A Unique On-line Method to Infer Black Carbon Contributions to Water-Insoluble Contributions. *Aerosol Sci. Technol.*, 48(23):706–714.
- Short, D., Vu, D., Durbin, T. D., Karavalakis, G., and Asa-Awuku, A. (2015a). Particle Speciation of Emissions from Iso-Butanol and Ethanol Blended Gasoline in Light-Duty Vehicles. *J. Aerosol Sci.*, 84:39–52.
- Short, D., Vu, D., Durbin, T. D., Karavalakis, G., and Asa-Awuku, A. (2015b). Components of Particle Emissions from Light-Duty Spark-Ignition Vehicles with Varying Aromatic Content and Octane Rating in Gasoline. *Environ. Sci. Technol.*, 49(17):10682–10691.
- Storey, J. M., Barone, T., Thomas, J., and Huff, S. (2012). Exhaust Particle Characterization from Lean and Stoichiometric DI Vehicles Operating on Ethanol-Gasoline Blends. *SAE Technical Paper 2012-01-0437*.
- Storey, J. M., Lewis, S., Szybist, J., Thomas, J., Barone, T., Eibl, M., Nafziger, E., and Kaul, B. (2014). Novel Characterization of GDI Engine Exhaust for Gasoline and Mid-level Gasoline-Alcohol Blends. *SAE Technical Paper 2014-01-1606*.
- Solomon, A. S., Anderson, R. W., Najt, P. M., and Zhao, F. (2000). Direct Fuel Injection for Gasoline Engines. *SAE Technical Paper PT-80*.
- Transportation and Climate Division. (2013). *Light-Duty Automotive Technology, Carbon Dioxide Emissions, and Fuel Economy Trends: 1975 through 2012*. EPA Report EPA-420-R-13-001, US EPA Office of Transportation and Air Quality, Washington, DC.
- Turpin, B. J., and Lim, H. (2001). Species Contributions to PM 2.5 Mass Concentrations: Revisiting Common Assumptions for Estimating Organic Mass. *Aerosol Sci. Technol.*, 35(1):602–610.
- Verma, V., Rico-Martinez, R., Kotra, N., King, L., Liu, J., Snell, T. W., and Weber, R. J. (2013). Contribution of Water-Soluble and Insoluble Components and Their Hydrophobic Subfractions to the Reactive Oxygen Species-Generating Potential of Fine Ambient Aerosols. *Environ. Sci. Technol.*, 46:11384–11392.
- Zhao, F., Lai, M.-C., and Harrington, D. L. (1999). Automotive Spark-Ignited Direct-Injection Gasoline Engines. *Prog. Energy Combust. Sci.*, 25:437–562.